PLASMA TURBULENCE AND STOCHASTIC ACCELERATION IN SOLAR FLARES

Vahé Petrosian[1],

Center for Space Science and Astrophysics, Stanford University, Stanford, CA 94305

ABSTRACT

Observational aspects of solar flares relevant to the acceleration process of electrons and protons are reviewed and it is shown that most of these observations can be explained by the interaction with flare plasma of a power law energy distribution of electrons (and protons) that are injected at the top of a flaring loop, in the so-called thick target model. Some new observations that do not agree with this model are described and it is shown that these can be explained most naturally if most of the energy released by the reconnection process goes first into the generation of plasma turbulence, which accelerates, scatters and traps the ambient electrons near the top of the loop stochastically. The resultant bremsstrahlung photon spectral and spatial distributions agree with the new observations. This model is also justified by some theoretical arguments. Results from numerical evaluation of the spectra of the accelerated electrons and their bremsstrahlung emission are compared with observations and shown how one can constrain the model parameters describing the flare plasma and the spectrum and the energy density of the turbulence.

1. INTRODUCTION

Because of the proximity of the Sun, solar flares have been detected in multitude of ways and there is considerable body of relatively detailed observations, a fact uncommon in other similar astrophysical sources and situations. Consequently, solar flares provide an excellent labaratory for testing ideas and models for all aspects of high energy astrophysical phenomena such as enenrgy generation and release, acceleration of particles and radiation processes. In this paper I describe a somewhat new paradigm for particle acceleration in solar flares where plasma waves or turbulence play a much more dominant role than has been attributed to them in the past. In §2 I present a brief review of some of the observational features of solar flares most relevant to the acceleration process, and a short outline of current ideas on production (and channels of release) of flare radiations. Then in §3 I describe some new observations that cannot easily be accounted for by the standard model, but can come about naturally in a model where particles are accelerated stochastically by plasma turbulence. Here I also give some theoretical justifications for such a model. In §4 I develop a simplified model of acceleration based on this idea and in §5 compare the predictions of this model with the new observations. In §6 I give a brief summary.

2. A BRIEF REVIEW

Flare radiation has been observed throughout the whole range of electromagnetic spectrum from long wavelength radio waves to gamma-rays up to hundreds of Mev. At radio wavelengths there are the various

---

[1]also Departments of Physics and Applied Physics

types (II, III, IV, V) of long wavelength emissions, but most relevant to the acceleration process is the continuum emission in the microwave-submillimeter range. Notable in the optical UV range are the H_α and white light emissions. In the soft X-ray range (< 10 keV), there is the thermal continuum emission and line emission by highly ionized heavy elements. Above 10 keV, in the hard X-ray (10 keV to 1 MeV) and gamma-ray (> 1 MeV) range, there is a non-thermal continuum radiation resulting from bremsstrahlung of the accelerated electrons, and in the 1 to 7 MeV range there is the gamma-ray line emission produced by accelerated protons and other ions. In addition to the electromagnetic radiation, there are other observations of flare phenomenon, among which the one most relevant to the acceleration process is the direct observation near the earth of accelerated electrons, protons, neutrons and other nuclei.

These radiations can be divided into two categories. The microwave, hard X-ray and all gamma-ray radiations are non-thermal radiation produced directly by the accelerated particles and constitute what is called the *impulsive phase* of the flares. These radiations are highly correlated and often show almost identical temporal evolution. The rest of the radiations are associated with what is called the *gradual phase* of the flare and are manifestations of flare plasma energized by the primary energy release process. These secondary radiations evolve at a rate that is approximately proportional to the integral of the impulsive time profiles, achieve their maximum at the end of the impulsive phase and then decay gradually.

Initially when only thermal radiation was observed, it was believed that most of the released energy goes directly into heating. But since the discovery of the non-thermal microwave and hard X-ray radiation it is believed that a large fraction, perhaps all, of the flare energy goes into acceleration of particles, mostly electrons with a power law distribution, $f(E) = \kappa E^{-\delta}$. These electrons produce X-rays through collisions with the ambient protons and ions as they travel down the flaring loop. Some of the radiation comes from the loop but the bulk of it is emitted in the high density regions below the transition layer. The total bremsstrahlung yield of X-rays with energy $k \geq E_0$ (in units of $m_e c^2$) is $Y = \frac{2\pi\alpha}{\ln\Lambda} \frac{E_0 \delta - 1}{\delta^2(\delta-2)}$, where α is the fine structure constant and $\ln\Lambda \simeq 20$ is the Coulomb logarithm. For typical values of $E_0 = 20$ keV and $\delta = 4$, $Y \leq 10^{-5}$. This means that almost all of the accelerated electron energy goes into heating or evaporation of plasma in the lower atmosphere, which gives rise to the softer X-rays and other gradual thermal radiations. This scenario agrees with the above-mentioned integral relation, the usual power law X-ray spectra, and the rudimentary observations of the spatial structure (double foot point sources) observed at hard X-rays by SMM and HINATORI spacecrafts.

The electrons as they spiral down the flaring loop (defined by the magnetic lines of force) emit also synchrotron radiation at microwave frequencies. The interpretation of this emission is more complicated because of its dependence on the magnetic field strength and geometry, and the presence of various kinds of absorptions. Accelerated protons and ions give rise to nuclear excitation and other gamma-ray lines in the 1-7 MeV range and to a continuum emission around 50 MeV from decay of pions they produce. For a review of gamma-rays from protons and ions the reader is referred to the excellent review by Ramaty and Murphy (1989). We shall not discuss the microwave emissions nor describe the models for gamma-ray line emission whose presence complicates the interpretation of the electron bremsstrahlung emission. To avoid this complication we will deal with the so-called electron dominated flares where a small number of ions are accelerated and their emission can be ignored (cf. e.g. Marschhaüser et al. 1991).

3. WHY PLASMA TURBULENCE?

There are, however, several more recent observations which do not agree with this scenario at least in its simplest form. In this section we describe two such observations and show how the presence of plasma turbulence can account for these observations. Then we present some theoretical arguments in favor of a model where bulk of the energy released by the reconnection process does not go directly into heating of the plasma or acceleration of the particles but into generation of plasma waves or turbulence which in turn can accelerate particles and heat the plasma (directly, or indirectly via the accelerated particles).

3.1. Observational Motivation

The two observations that provide evidence for the above scenario are the wide dynamic range spectral and high spatial resolution hard X-ray observations. There may be other evidence such as the impulsive soft X-ray observation from foot points (Hudson et al. 1994, Petrosian 1994, 1996).

3.1.1. Spectral Evidence

Observed spectra over a limited range (30-500 keV) can be fitted to bremsstrahlung spectra emitted by electrons with a power law energy spectrum. But higher resolution spectra, especially those with a wider dynamic range (10 keV to 100 MeV), observed by the gamma-ray spectrometer (GRS) onboard SMM and by the combined BATSE and EGRET instrumentS on Compton Gamma-Ray Observatory (CGRO), show considerable deviation from a simple power law; as shown in Figure 1, there is spectral hardening (flatter spectra) above around few 100s of keV and a steep cutoff above 40 MeV. These kinds of deviations can be produced by the action of Coulomb collisions and synchrotron losses during the *transport* of the electrons from top of a loop to the foot points. However, as shown by Petrosian, McTiernan & Marshhaüser (1994), the observed deviations would require plasma densities n and magnetic fields B, which are much higher than those believed to be present (see Figure 1). We conclude that these signatures must be present in the spectra of the accelerated electrons. As we shall show in §5 the stochastic acceleration model described in the next section can reproduce these observations with more reasonable values of the parameters.

3.1.2. Spatial Structure

The second observation which provides a more direct evidence for presence of turbulence at the top of loops is the observations by YOHKOH of loop top hard X-ray (10-50 keV) emission (Masuda et al. 1994, Masuda 1994). Figure 2 shows an image of one such flare along with variations with time of the emission intensities from the loop top, the foot points and their ratio. Several other flares show similar images and emission ratios. There exists also a limited spectral information (Masuda 1994 and Alexander & Metcalf 1997).

In the standard thick target model, the spatial variation of the bremsstrahlung emission depends primarily on the relative values of the length L of the loop and the Coulomb collision mean free path, $\lambda_{\text{Coul}} = \beta^2 E/(4\pi r_0^2 n \ln\Lambda)$, where $\beta = v/c$ is the electron velocity in units of the speed of light and $r_0 \simeq 2.8 \times 10^{-13}$cm is the classical electron radius. In general, $L \ll \lambda_{\text{Coul}}$ in the corona so that most particles travel through the coronal portion of the loop freely but undergo rapid collision and bremsstrahlung

emission once they reach the transition region and the chromosphere where the density increases by several orders of magnitude within a much shorter distance. Loop top emission is possible only if $\lambda_{\rm Coul} \ll L$, in which case the accelerated electrons lose most of their energy at the top of the loop with no emission from foot points. If $\lambda_{\rm Coul} \simeq L$ then one would expect a uniform emission from throughout the loop. For further deatails see J. Leach's Ph.D. thesis (1984), Fletcher (1995) and Holman (1996).
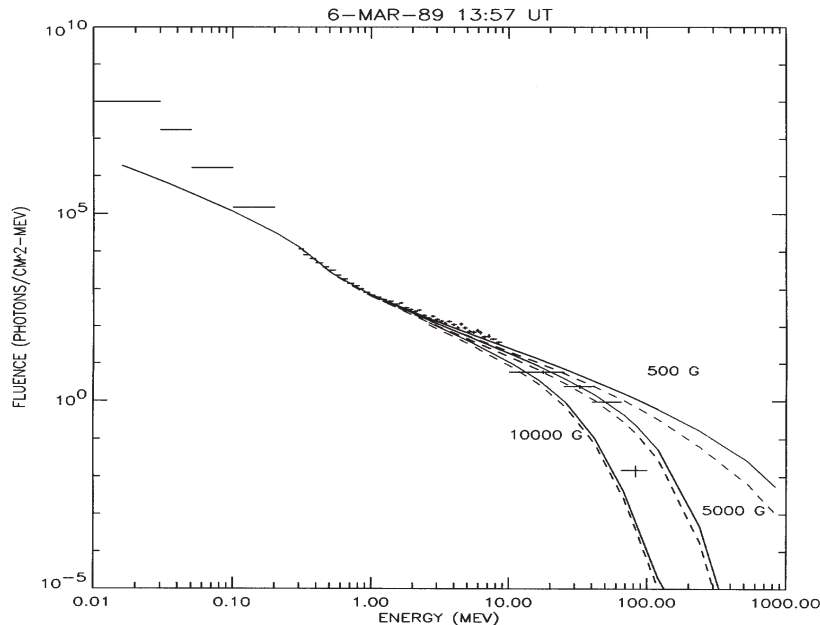

Fig. 1.— Spectrum of the first impulsive bump (13:57:29-13:58:34 UT) of the 1989 March 6 electron dominated flare. The solid lines show the whole loop spectrum for an injected power law electrons (index $\delta = 2.2$) adjusted to obtain best fit in 0.3-10 MeV range. The curves are marked by the value B_0 at the top of the loop with a factor of 2.5 increase at the transition region. The dashed lines show the effects of the optical depth. Note the failure of the models at low energies and the high required field strengths at high energies. (From Petrosian et al. 1994.)

Significant loop top emission is possible if the loop is highly inhomogeneous. Since the emission is proportional to the ambient density a higher density at the loop top can mimic the observed variation (Wheatland and Melrose 1995). However, it is difficult to see how large density gradients can be maintained in a $T \geq 10^6$ K plasma. Enhancement of loop top emission can be produced more naturally in loops with converging field geometry. The field convergence increases the pitch angle of the particles as they travel down the loop, and if strong enough, can reflect them back up the loop before they reach the transition region. This increases the density of the accelerated electrons near the top of the loop giving rise to a corresponding enhancement of the bremsstrahlung emission. Such models were also investigated by Leach (1984), show significant increases of emission from loop tops for large convergence ratio (see also Leach & Petrosian 1983 and Figures 1 and 2 in Peterosian & Donaghy 1999; **PD** for short), and by Fletcher (1996) showing increase in the average height of the X-ray emission.
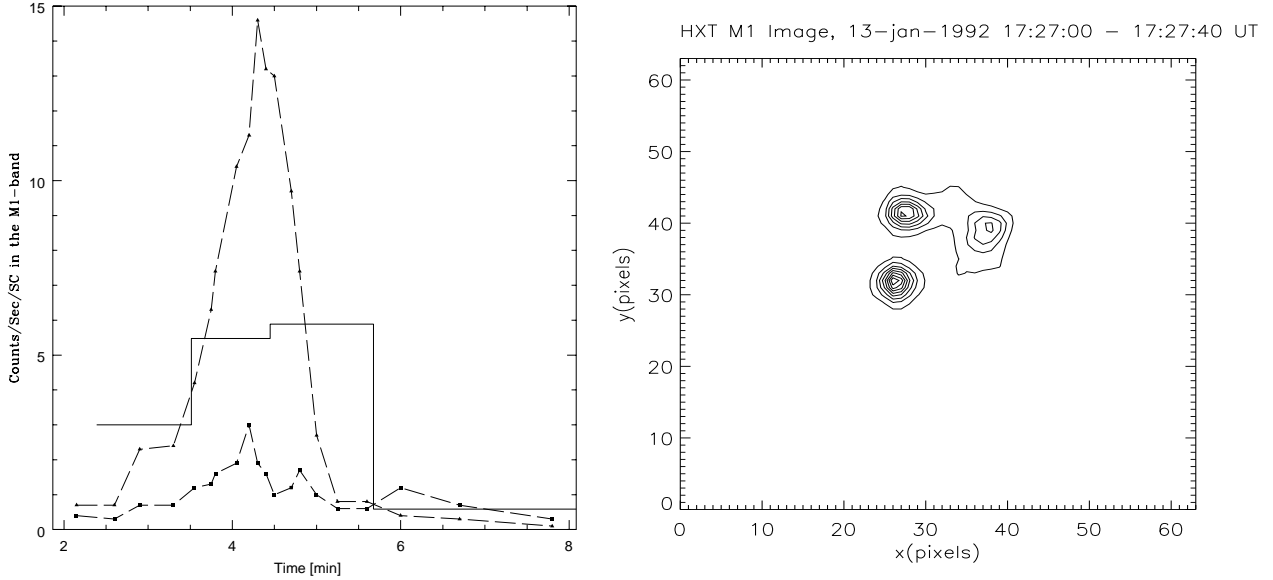
Fig. 2.— *Left panel* shows the intensities of the foot points (top dashed curve), the loop top (lower dashed curve) and their ratio (solid histogram). *Right panel* shows the contour plots of these sources for January 13 1991 flare. Taken from Masuda 1994.

Finally, trapping of electrons near the top of a loop can come about by an enhanced pitch angle scattering with a mean free path $\lambda_{\mathrm{scat}} \ll L \ll \lambda_{\mathrm{Coul}}$. In this case electrons will undergo many pitch angle scatterings and achieve an isotropic pitch angle distribution before they escape within a time $T_{\mathrm{esc}} \simeq \frac{L}{v} \times \frac{L}{\lambda_{\mathrm{scat}}} \gg \frac{L}{v}$. It can be shown that the ratio of the loop top emission to emission from other parts of the coronal portion of the loop (i.e. the legs of the loop, which do not contain such a scattering agent but are of comparable length) will be approximately $J_{LT}/J_{Loop} \simeq L/\lambda_{\mathrm{scat}}$, in which case we may detect emission only from the top of the loop and the high density foot points, but not from the legs of the loop. A possible scattering agent which could satisfy this condition is plasma turbulence. If this is the case, however, one must also include the possibility of acceleration of the particles by the same plasma turbulence.

3.2.   Theoretical Arguments

Various mechanisms have been proposed and are investigated for the acceleration of particles in all kinds of astrophysical situations (see, e.g. review articles in the Proc. of IAU Colloq. 142, 1994, ApJ Suppl. 90). The three most common mechanisms are the following.

Electric Fields parallel to the magnetic field lines can accelerate charged particles. For fields greater than the Dreicer field, $\mathbf{E}_D = kT/(e\lambda_{\mathrm{Coul}})$, particles of charge e gain energy faster than the mean collision time $\tau_{\mathrm{Coul}} = \lambda_{\mathrm{Coul}}/v$. This can lead to unstable particle distribution, which in turn can give rise to turbulence and cause mostly heating (Boris et al. 1970, Holman 1985). Sub-Dreicer fields, in order to accelerate charged particles to relativistic energies, must extend over a region $L \gg \lambda_{\mathrm{Coul}}$, which as pointed above cannot be the case for a loop size acceleration region. An anomalously large resistivity is one way to

get around this difficulty (Tsuneta 1985). It seems that some other mechanism is required for acceleration to MeV and GeV ranges (needed for electrons and protons, respectively).

Shocks are the most commonly considered mechanism of acceleration because they can quickly accelerate particles to very high energies. However this requires the existence of some scattering agent to force repeated passage of the particles across the shock. The most likely agent for scattering is plasma turbulence or plasma waves. The rate of energy gain then is governed by the scattering rate which in this case is proportional to the pitch angle diffusion coefficient $D_{\mu\mu}$. However, the turbulence needed for the scattering can also accelerate particles stochastically (a second order Fermi process) at a rate D_{EE}/E^2, where D_{EE} is the energy diffusion coefficient. At high energies $D_{\mu\mu} \gg D_{EE}/E^2$ favoring shock acceleration.

Stochastic Acceleration is favored for acceleration of low energy background particles because several recent analyses by Hamilton & Petrosian 1992 and Dung & Petrosian 1994, and by Miller and collaborators (e.g. Miller & Reames 1996, Schlickeiser & Miller 1998) have shown that under correct conditions plasma waves can accelerate low energy particles within the desired times. More importantly, as our more recent work has shown (Pryadko & Petrosian 1997), at low energies the above inequality is reversed, $D_{EE}/E^2 \gg D_{\mu\mu}$, so that the stochastic acceleration (rate $\propto D_{EE}/E^2$) becomes more efficient than shock acceleration whose rate is governed by the smaller coefficient $D_{\mu\mu}$. *Thus, low energy particles are accelerated more efficiently stochastically than by shocks.*

We can, therefore, imagine two scenarios. In one scenario, low energy particles are accelerated first by electric fields (or stochastically) and then to higher energies by shocks. In a second simpler scenario, stochastic acceleration by turbulence does the whole process, accelerating the background particles to high energies (cf. Petrosian 1994). We now describe the second scenario for flares.

4. STOCHASTIC ACCELERATION

Stochastic acceleration by turbulence was first proposed by Ramaty and collaborators (see e.g. Ramaty 1979 and Ramaty & Murphy 1987) for solar flare protons and ions. As argued above this process appeares to be the most promising process for acceleration of flare electrons as well (see also Petrosian 1994 and 1996). Similar arguments have been put forth by Schlickeiser and collaborators (Schlickeiser 1989; Bech et al. 1990), and Miller and collaborators (Miller 1991; Miller, LaRosa & Moore 1996; Miller, Guessoum & Ramaty 1990).

For the purpose of comparison with the observations mentioned above we need the energy spectrum and spatial distribution of the acceleraterd electrons. The exact evaluation of this requires solution of the time dependent coupled kinetic equations for *waves and particles*. This is beyond the scope of this work and is not warranted for comparison with the existing data. We therefore make the following simplifying and somewhat justifiable assumptions.

We assume that the flare energizing process, presumably magnetic reconnection, produces plasma turbulence throughout the impulsive phase at a rate faster than the damping time of the turbulence, so that the observed variation of the impulsive phase emissions is due to modulation of the energizing process. This assumption decouples the kinetic equation of waves from that of the electrons. We also assume that the turbulence is confined to a region of size L near the top of the flaring loop where particles undergo scattering and acceleration, but eventually escape within a time $T_{\rm esc} \simeq (1 + (L/\lambda_{\rm scat}))\tau_{tr}$, where $\lambda_{\rm scat} \propto 1/D_{\mu\mu}$ and $\tau_{tr} \simeq L/v$ is the traverse time across the acceleration region. Since both these times are

shorter than the observational integration time, we can use the steady state equation. And because the loop top emission requires $\lambda_{\mathrm{scat}} \ll L$, we can assume isotropy of the pitch angle distribution and evaluate the electron spectrum integrated througout the finite acceleration site. The kinetic equation then simplifies to

$$\frac{\partial^2}{\partial E^2}[D(E)f] - \frac{\partial}{\partial E}[(A(E) - |\dot{E}_L|)f] - \frac{f}{T_{\mathrm{esc}}(E)} + Q(E) = 0. \tag{1}$$

Here D and A are the diffusion and systematic acceleration coefficients due to the stochastic process that are obtained from the standard Fokker-Planck equation and are related to the coefficient D_{EE} and

$$\dot{E}_L = \dot{E}_{\mathrm{Coul}} + \dot{E}_{\mathrm{synch}} = -4\pi r_0^2 cn \ln \Lambda/\beta - 4r_0^2 B^2 \beta^2 \gamma^2/9m_e c \tag{2}$$

describes the Coulomb and synchrotron energy loss rates (in units of $m_e c^2$). For the source function, $Q(E)$, we use a Maxwellian distribution with temperature, $kT = 1.5$ keV.

Following our earlier formalism (Hamilton & Petrosian 1992, Park, Petrosian & Schwartz 1997, **PPS** for short) we use the following parametric forms for the diffusion coefficients.

$$D(E) = \mathcal{D}\beta(\gamma\beta)^{q'}, \;\; A(E) = \mathcal{D}(q'+2)(\gamma\beta)^{q'-1}, \;\; T_{\mathrm{esc}}(E) = \mathcal{T}_{\mathrm{esc}}(\gamma\beta)^s/\beta + L/(\beta c\sqrt{2}). \tag{3}$$

Here q' is related to q, the spectral index of the (assumed) power law distribution for the plasma wave vectors. The above forms are more general than what one obtains from a single type of plasma waves, say the whistler waves (where $\mathcal{D}$ and $\mathcal{T}_{\mathrm{esc}}$ are related and $s = q' = q - 2$). They can accomodate other scattering processes, such as the hard sphere model ($q' = 2, s = 0$, see Ramaty 1979) or more general turbulence. For a more general spectrum of turbulence that includes all possible waves, more accurate numerical values are obtained by Dung & Petrosian (1994) and Pryadko & Petrosian (1997, 1999). For a more complete analysis one should use these numerical results. The existing data do not warrant considerations of such details. However, we shall choose the parameters in the above expressions so that the relevant parameters qualitatively behave like the ones from these numerical results. As shown in these papers, the rate of acceleration $\mathcal{D}$ and escape time $\mathcal{T}_{\mathrm{esc}}$ are proportional to the electron gyrofrequency, Ω_e, and the level of turbulence $f_{turb} = 8\pi\mathcal{E}_{tot}/B^2$, where $\mathcal{E}_{tot}$ is the total energy density of turbulence.

We solve equation (1) numerically for the spectrum of electrons at the acceleration site, $f_{AS}(E)$, and then evaluate the (*thin target*) bremsstrahlung spectrum, number of photons as a function of photon energy k (in units of $m_e c^2$), emitted by these electrons:

$$J_{AS}(k) = V \int_k^\infty dE f_{AS}(E) \beta c n_{AS} \frac{d\sigma}{dk}(E, k), \tag{4}$$

Here V and n_{AS} are the volume and the background density in the acceleration site, $d\sigma/dk$, given by Koch & Motz (1959, eq. [3BN]), is the relativistically correct, angle integrated, bremsstrahlung cross section. The electrons escaping the acceleration site travel to the foot points and maintain a nearly isotropic pitch angle distribution in the downward direction with a spectral flux equal to $F_{\mathrm{esc}} = Lf_{AS}/T_{\mathrm{esc}}$ and emit bremsstrahlung at the foot points. As is well known (see, e.g. Petrosian 1973), the effective spectrum of the electrons (the so-called cooling spectrum) in the *thick target* foot point sources is

$$f_{\mathrm{thick}}(E) = -\frac{1}{\dot{E}_L} \int_E^\infty \frac{f_{AS}(E)}{T_{\mathrm{esc}}} dE, \tag{5}$$

so that the photon spectrum at the foot points, $J_{FP}(k)$, is obtained from equation (4) by replacing the above spectrum for f_{AS}.

For a steep power law electron spectrum, ($f(E) = \kappa E^{-\delta}, \delta \gg 1$), and for a relatively slow variation with energy E of T_{esc} (i.e. small s), one can obtain simple analytic expressions for the photon spectra. For example, the ratio of the foot point to loop top emissions can be approximated by the simple expression

$$\frac{J_{FP}}{J_{AS}} \simeq \frac{\tau_{\text{Coul}}(k)}{T_{\text{esc}}(k)} = (4\pi r_0^2 c n_{AS} \ln \Lambda \mathcal{T}_{\text{esc}})^{-1} \begin{cases} 2^{(2-s)/4} k^{2-s/2} & k \ll 1, \\ k^{1-s} & k \gg 1, \end{cases} \tag{6}$$

where the Coulomb collision time is given by

$$\tau_{\text{Coul}}(k) \equiv -\left(\frac{E}{\dot{E}_{\text{Coul}}}\right)_{E=k} = (4\pi r_0^2 \ln \Lambda n_{AS} c)^{-1} \begin{cases} \sqrt{2} k^{3/2} & k \ll 1, \\ k & k \gg 1. \end{cases} \tag{7}$$

Steep spectra are obtained for slow acceleration rates (low levels of turbulence) or rapid escapes, but in the opposite case, for larger values of $\mathcal{DT}$, the electron spectra become flat up to some high energy, E_{synch}, where sychrotron losses come in and the spectrum falls off rapidly. In this case the above ratio is modified by setting $k = E_{\text{synch}}$. For more details see PD.

5. COMPARISON WITH OBSERVATIONS

5.1. High Resolution Total Spectra

The high resolution and wide dynamic range spectra are available only for the total emission and not for the loop top and foot point sources separately. We combine the two spectra and fit $J = J_{FP} + J_{LT}$ to the observed spectra of electron dominated flares from GRS on SMM and BATSE-EGRET on CGRO. Figure 3 and Table 1 show these fits and the values of the model parameters obtained for three different forms for the acceleration coefficients. As evident the simple hard sphere model fails to reproduce the spectra and can be easily ruled out. But for a model based on the whistler waves and a more general model, we obtain very good fits and reasonable values of the parameters. The values for density are somewhat larger than those assumed usullay, but the required magnetic field and amount of turbulence, f_{turb}, are very reasonable. Similar parameter values are obtained for two other electron dominated flares (see PPS).

5.2. High Spatial Resolution Data

The best high spatial resolution flare data in the hard X-ray range are those mentioned in §3 and shown in Figure 2. In Figure 4 we show model predictions for the intensity ratio J_{FP}/J_{LT} and the spectal indices obtained by a power law fit to the spectra over the short range, 20 to 50 keV, as a function of the acceleration rate $\mathcal{D}$ and for several values of the important parameters, such as density, magnetic field, and escape time. The ranges of the observed values for these quantities obtained by Masuda (1994) and Alexander & Metcalf (1997) are shown by the horizontal dotted lines.

As evident from Figure 4 some of the values of the model parameters can be constrained by the observations. For high ambient densitites ($n \simeq 10^{11}$cm $^{-3}$) the observed ratios agree with a wide range of the acceleration rate except for short escape times. But at lower densities only smaller values of the acceleration rate are acceptable. On the other hand, a stronger constrain can be obtained from consideration of the spectral indices, which require a slow acceleration rate, $\mathcal{D} < 0.15$s, and show a weak dependence on the ambient density and escape time $\mathcal{T}_{\text{esc}}$. There is also some dependence on the exponents q' and s (not
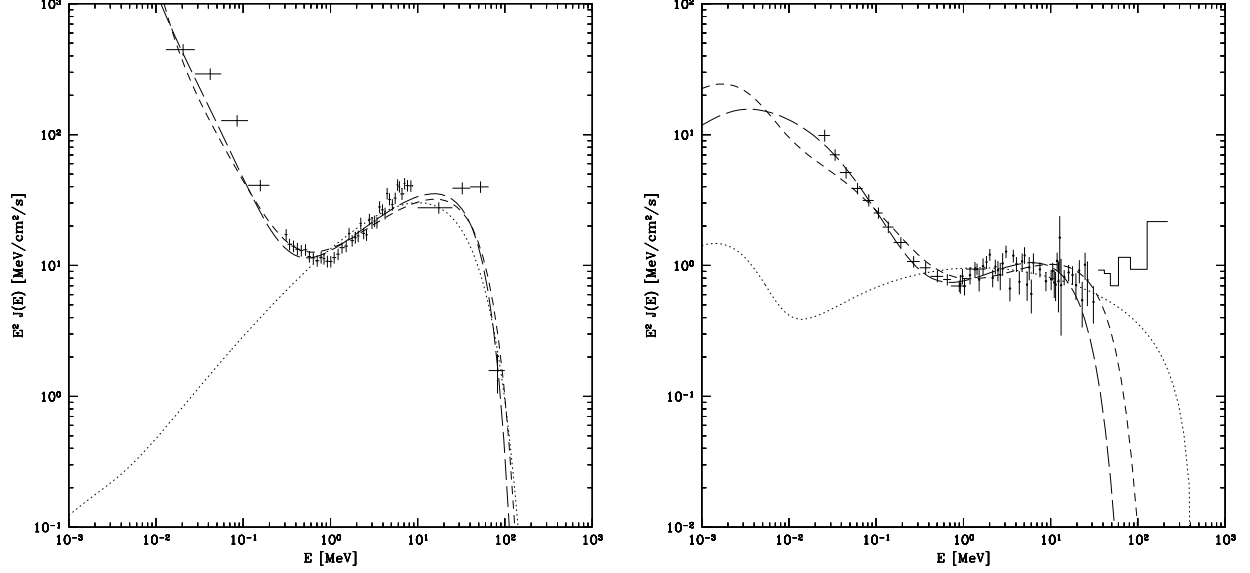
Fig. 3.— Comparison of the observed spectra with the total (foot point plus loop top) photon power spectra ($E^2J(E)$): Hard sphere (short dashed line), whistler (medium dashed line), and the general (long dashed line). *Left panel* for the first 1989 March 6 impulsive burst (UT 13:57:29 – 13:58:34) from GRS shown in Fig. 1. The fitted parameter are given in Table (1) below. *Right panel* for the BATSE (cross hair) and EGRET (solid bullet with vertical error bars) data of the 1991 June 30 flare (UT 2:55:32 – 2:57:11). The solid histogram at high energy is the EGRET 2-σ upper limits. The fitted parameters for this and two other electron dominated flares are similar to those in Table (1). For further details see PPS.

Table 1:   Model parameters for the first impulsive peak of the 1989 March 6 electron dominated flare.

parameters	hardsphere	whistler	general
$Q_0[\mathrm{cm^{-3}s^{-1}}]$	$(1.4 \pm 0.1) \times 10^8$	$(1.7 \pm 0.1) \times 10^{13}$	$(7.7 \pm 5.1) \times 10^{12}$
$n[\mathrm{cm^{-3}}]$	$(7.5 \pm 0.1) \times 10^{10}$	$(2.9 \pm 0.1) \times 10^{11}$	$(1.62 \pm 0.43) \times 10^{11}$
$B[\mathrm{G}]$	2007 ± 29	500 ± 40	325 ± 66
q'	2	1.45 ± 0.02	1.22 ± 0.09
s	0	q'	1.87 ± 0.14
$\mathcal{T}[\mathrm{s}]$	1.38 ± 0.03	0.12	$0.090 \pm .006$
$L[\mathrm{cm}]$	10^9	$(2.8 \pm 0.4) \times 10^9$	10^9
f_{turb}		7×10^{-6}	
ν	45	44	43
χ^2/ν	15	6.1	4.9

shown here) and essentially no dependence on the value of the magnetic field B whose effect come in above MeV photon energies. The parameters from this comparison are in agreement with those given in Table 1 obtain from spectral fittings to different flares. For further details the reader is referred to PD.
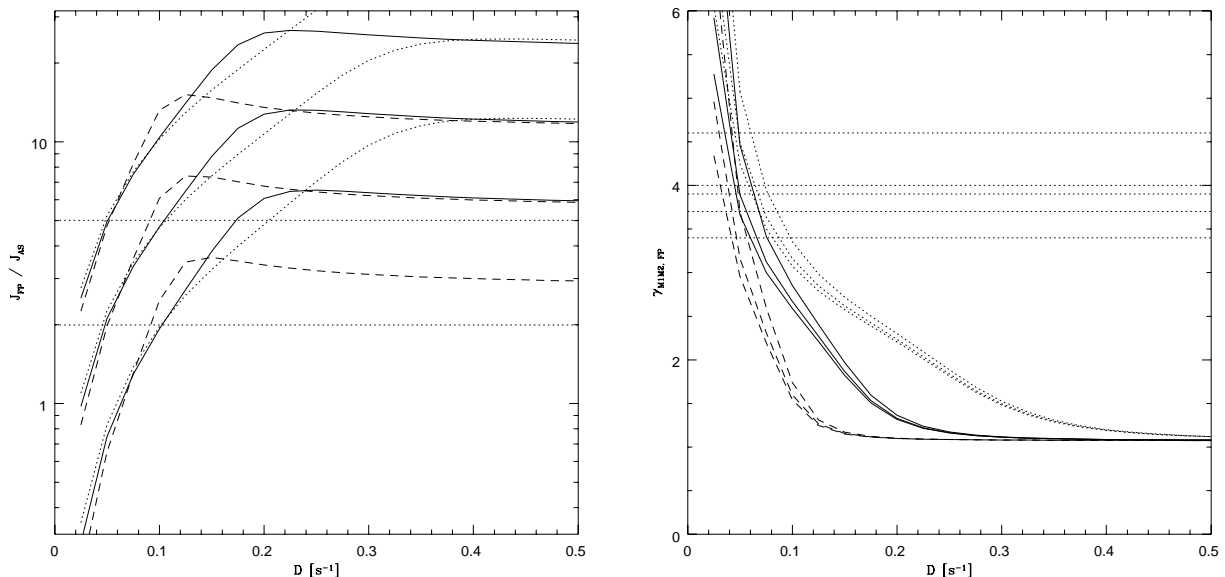

Fig. 4.— *Left panel*: The ratio J_{FP}/J_{LT} in the 23 to 33 keV range (the M1 band) as a function of $\mathcal{D}$ for three escape times $\mathcal{T}_{esc} = 0.05, 0.1$ and 0.2 s; dotted, solid and dashed lines, respectively, and for three values of density $n/(10^{10}\text{cm}^{-3}) = 2.5, 5$ and 10; in each case from top to bottom, respectively. The magnetic field $B = 300$G, $s = 1.5$ and $q' = 1.7$. The horizontal dotted lines show the range of the observed ratios. *Right panel*: The photon number spectral index ($\gamma = -d\ln J(k)/d\ln k$) between channels M1 and M2 for the foot point sources. Note that the order of the densities here is the opposite of that in the left panel, increasing from bottom to top. The horizontal dotted lines show the observed values of this index. From PD.

6. SUMMARY

I have shown that some recent observations do not agree with the predictions of the standard thick target model for the impulsive phase of solar flares. I have demonstrated that higher resolution spectral observations over a wide dynamic range and some high spatial resolution observations in the hard X-ray regime can be explained by a modification of the standard model where the electrons are accelerated stochastically by plasma turbulence. Based on models obtained in PPS and PD, I have shown that the resultant model parameters are reasonable. A more accurate determination of the validity of the model and the range of its parameters can be obtained with simultaneous high spectral and spatial resolution observation of many flare that is expected during the upcoming solar maximum from HESSI, a new mission to be launched some time in 2000.

REFERENCES

Alexander, D., & Metcalf, T. R. 1997, ApJ, 489, 442

Bech, F.-W., Steinacker, J., & Schlickeiser, R. 1990, Sol. Physics, 129, 195

Boris, J. P., Dawson, J. M. & Orens, J. H. 1970, Phys. Rev. Lett., 25, 706

Dung, R., & Petrosian, V. 1994, ApJ, 421, 550

Fletcher, L. 1995, A&A (Letters), 303, L9

Fletcher, L. 1996, A&A , 310, 661

Hamilton, R. J., & Petrosian, V. 1992, ApJ, 398, 350

Holman, G. 1985, ApJ, 293, 584

Holman, G. 1996, BAAS, 28, 939

Hudson, H. S. et al. 1994, ApJ Letters, 422, L25

Koch, H. W., & Motz, J. W. 1959, Rev. Mod. Phys., 31, 950

Leach, J. 1984, Ph. D. Thesis, Stanford University

Leach, J., & Petrosian, V. 1983, ApJ, 269, 715

Marschhäuser, H. et al. 1994, AIP Conf. Proc. 294, eds. J. M. Ryan & W. T. Vestrand, 171

Masuda, S. 1994, Ph.D. Thesis, The University of Tokyo

Masuda, S. et al. 1994, Nature, 371, 455

Miller J.A. 1991, ApJ. 376, 342

Miller, J. A., Guessoum, N., & Ramaty, R. 1990, ApJ, 361, 701

Miller, J. A., LaRosa, T. N., & Moore, R. L. 1996, ApJ, 445, 464

Park, B. T., Petrosian, V., & Schwartz, R. A. 1997, ApJ, 489, 358 (**PPS**)

Petrosian, V. 1973, ApJ, 186, 291

Petrosian, V. 1994, AIP Conf. Proc. 294, eds. J. M. Ryan & W. T. Vestrand, 162

Petrosian, V. 1996, AIP Conf. Proc. 374, eds. R. Ramaty, N. Mandzhavidze & X-M. Hua, 445

Petrosian, V., & Donaghy, T. Q. 1999, ApJ, 527, in press, Dec. 20, (astro-ph/9907181) (**PD**)

Petrosian, V., McTiernan, J. M., & Marschhäuser, H. 1994, ApJ, 434, 747

Pryadko, J., & Petrosian, V. 1997, ApJ, 482, 774

Pryadko, J., & Petrosian, V. 1999, ApJ, 515, 873

Ramaty, R. 1979, AIP conf. proc., No. 56, eds. J. Arons, C. Max & C. McKee 1987, 135

Ramaty, R., & Murphy, R. J. 1987, Space Sci. Rev., 45, 213

Schlickeiser, R. 1989, ApJ, 336, 243

Schlickeiser, R. & Miller, J. A. 1998, ApJ, 492, 352

Tsuneta, S. 1985, ApJ, 290, 353

Wheatland, M. S., & Melrose, D. B. 1995, Sol. Physics, 185, 283